

Hf isotope constraints on mantle evolution

Vincent J.M. Salters^{a,*}, William M. White^b

^a National High Magnetic Field Laboratory and Department of Geology, Florida State University, 1800 E Paul Dirac Drive, Tallahassee, FL 32306, USA

^b Department of Geosciences, Cornell University, Snee Hall, Ithaca, NY, USA

Received 20 January 1997; revised 29 September 1997; accepted 4 October 1997

Abstract

The similarity of the Lu–Hf and Sm–Nd isotope system during most mantle differentiation processes makes the combination of $^{176}\text{Hf}/^{177}\text{Hf}$ and $^{143}\text{Nd}/^{144}\text{Nd}$ a very sensitive indicator of a select number of processes. This paper presents new Hf-isotope data for a large number of ocean islands and examines the Hf–Nd–Pb isotope relations of oceanic volcanics. Except for HIMU islands, St. Helena and Tubaii, the Hf and Nd isotope ratios in ocean island basalts (OIB) are extremely well correlated. It is argued that crustal recycling (by either continental or oceanic sediments) most likely did not cause the Hf–Nd variations. The correlated $^{176}\text{Hf}/^{177}\text{Hf}$ – $^{143}\text{Nd}/^{144}\text{Nd}$ variations in OIB most likely represent the time integrated fractionations which are the result of melting in the presence of garnet. The Hf-isotope systematics of HIMU-type OIB are consistent with these basalts representing recycled oceanic crust and thus support the earlier hypothesis on the origins of HIMU basalts. Chondrites form an array that is at high angle with the OIB array. This allows a choice in the $^{143}\text{Nd}/^{144}\text{Nd}$ and $^{176}\text{Hf}/^{177}\text{Hf}$ values for chondritic bulk earth. With a choice of bulk earth at the extreme end of the OIB array the shift of OIB to higher $^{176}\text{Hf}/^{177}\text{Hf}$ can be explained by either isolation of a significant amount of basalts from the mantle for several billions of years or by fractionation and isolation of small amounts (< 1%) of perovskite, during the early history of the Earth. The large range in Hf-isotopes for a limited range in Nd-isotopes in MORB can be explained by addition of small amounts (<< 1%) of the perovskite material back into the MORB mantle. If chondritic BE is chosen to be internal to the OIB, the well correlated Hf–Nd isotope characteristics in OIB argue against the fractionation of perovskite during the early history of the Earth and the shape of the MORB field remains an enigma. © 1998 Elsevier Science B.V. All rights reserved.

Keywords: Hf isotope constraints; Isotope constraints; Mantle evolution

1. Introduction

The advance of analytical techniques in the last five years has made the Hf-isotopes more applicable to a variety of problems. This paper reviews the limits the Hf-isotopes provide on some of the models for Earth evolution. One of the strongest constraints

on Earth evolution is provided by the combined variations in Hf and Nd isotope compositions. The Hf and Nd-isotope systematics are similar in that both parents; ^{176}Lu and ^{147}Sm respectively, are more compatible during melting than their daughters, ^{176}Hf and ^{143}Nd . Much of the constraints that the Lu–Hf system provides comes from the pioneering work of Patchett and co-workers (Patchett and Tatsumoto, 1980, 1981a,b; Patchett et al., 1981; Patchett, 1983a,b).

* Corresponding author.

Relatively few processes are able to fractionate the Lu–Hf system different than the Sm–Nd system and therefore the coherence (or lack of coherence) of $^{176}\text{Hf}/^{177}\text{Hf}$ with $^{143}\text{Nd}/^{144}\text{Nd}$ is a sensitive indicator of those processes. Decoupling of the two isotope systems is established during erosion and sedimentation (Patchett et al., 1984; White et al., 1986; Ben Othman et al., 1989) where Hf is mostly hosted by zircon. As zircon is a refractory mineral, the zircon with its high Hf content mostly ends up in sandstones and turbidites while red clays have higher Lu/Hf ratios.

In the shallow mantle, melting in the presence of garnet results in larger Lu/Hf fractionations (compared to Sm/Nd fractionations) than garnet absent melting and in some decoupling of Sm–Nd from the Lu–Hf system. The coherence between $^{176}\text{Hf}/^{177}\text{Hf}$ and $^{143}\text{Nd}/^{144}\text{Nd}$ can be used to deduce the time integrated importance of the processes that resulted in both fractionation and decoupling. The slope of the correlated array carries information on the time integrated Lu/Hf and Sm/Nd fractionation (Patchett, 1983b; Salters and Hart, 1991; Beard and Johnson, 1993). Deeper in the Earth's mantle fractionation or melting in the presence of perovskite can also fractionate Lu/Hf significantly different from Sm/Nd (Kato et al., 1988a,b; Salters and Hart, 1991).

An essential piece of information on the Hf-isotope systematics is the Hf-isotope composition of chondrites. The bulk earth $^{176}\text{Hf}/^{177}\text{Hf}$ value was based on a chondrites (Patchett and Tatsumoto, 1981b; Tatsumoto et al., 1981; Patchett, 1983b) and assumed a chondritic evolution of the Earth (as is assumed for Nd-isotopes). The chondritic $^{176}\text{Hf}/^{177}\text{Hf}$ ratio was recently updated by analyses of C, E and O chondrites (Blichert-Toft and Albarède, 1997) to $^{176}\text{Hf}/^{177}\text{Hf} = 0.282772 \pm 29$ and $^{176}\text{Lu}/^{177}\text{Hf} = 0.0332$. The new data resulted in a factor of four decrease in the uncertainty of the chondritic evolution line. This data was obtained while a value of 0.282163 was measured for the $^{176}\text{Hf}/^{177}\text{Hf}$ of standard JMC-475. This JMC-475 value is very close to the average JMC-475 value obtained by a variety of laboratories and we propose that all data will be reported relative to JMC-475 equals 0.282163. The new bulk earth (BE) value is shown in Fig. 1 and labeled as BE_{JBT} , whereby the subscript indicates the lineage of the estimate (J stands for Jacobsen and Wasserburg (1984) for the Nd-isotopic composition and BT stands for Blichert-Toft and Albarède (1997) for the Hf-isotopic composition).

An essential piece of information that will not be discussed further in this paper, is a study by Vervoort and co-workers (Vervoort and Patchett, 1996;

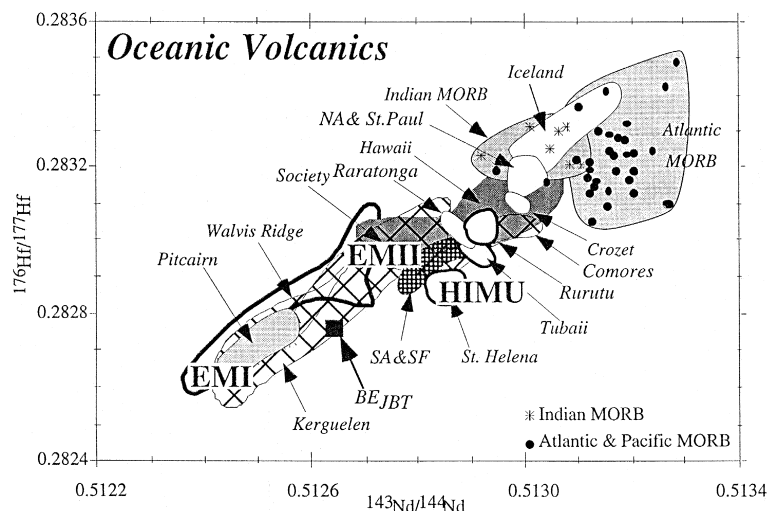


Fig. 1. Hf–Nd isotope correlation diagram of all oceanic volcanics. Additional data from (Patchett and Tatsumoto, 1980, 1981a; Patchett, 1983a,b; Stille et al., 1983, 1986; Hart et al., 1986; Salters and Hart, 1991; Salters, 1996). Stars are Atlantic and Pacific ocean ridge basalts and circles are Indian ocean ridge basalts.

Vervoort et al., 1996a) on Archean granites and gneisses. This study shows that the large fractionations in the Sm/Nd systems during the early history of the Earth as evidenced by high ϵ_{Nd} values in pre-3.0 Ga basic volcanics (Shirey and Hanson, 1986) are not accompanied by large Lu/Hf fractionations. The evidence now points towards disturbance of the Sm–Nd-system after crystallization. This new finding now eliminates the need for extensive fractionation of the early Earth and the formation of the majority (> 80%) of the continental crust during the first billion year of the Earth's history. Models in which the early Earth is extensively fractionated now have to involve very effective remixing as the early Archean mantle is relatively homogeneous (Vervoort et al., 1996b).

2. $^{176}\text{Hf}/^{177}\text{Hf}$ and $^{143}\text{Nd}/^{144}\text{Nd}$ variations in oceanic volcanics

Table 1 reports new data for ocean island basalts (OIB). This data was obtained with the intention to better determine the shape of the ocean island array on the Hf–Nd isotope correlation diagram (Fig. 1). With these additional analyses the OIB that define all the different endmembers in Sr–Nd–Pb isotope space (Zindler and Hart, 1986) have now been analyzed. The HIMU endmember is better defined with additional data from St. Helena, Tubaii and Rurutu, the EMI endmember is better defined through the addition of Pitcairn Hf-isotope data. In addition, the high $^{143}\text{Nd}/^{144}\text{Nd}$ -high $^{176}\text{Hf}/^{177}\text{Hf}$ -end of the OIB field is now better defined with additional analyses of basalts from Iceland, Ascension as well as high $^{143}\text{Nd}/^{144}\text{Nd}$ Indian Ocean island basalts. Additional mid-ocean ridge basalts (MORB) data now fill out the MORB field better although the shape of the field does not change.

The additional OIB data firms up the OIB field in Hf–Nd isotope space and results in small, but significant changes in its field. The majority of the OIB data fall in a tight array that encompasses the EMI endmember (Walvis Ridge, Pitcairn) at the low $^{176}\text{Hf}/^{177}\text{Hf}$ end of the array, the EMII endmember (internal to the array), and Iceland, Hawaii, Ascension, New Amsterdam and St. Paul forming the high $^{176}\text{Hf}/^{177}\text{Hf}$ end of the array. The high

$^{176}\text{Hf}/^{177}\text{Hf}$ -end of the OIB array ties in with the high $^{176}\text{Hf}/^{177}\text{Hf}$ -end of the MORB field. There are several first-order features in the Hf–Nd isotope variations in oceanic volcanics that constrain the evolution of their sources. First, the HIMU endmember, represented by St. Helena, Tubaii and Rurutu falls below the OIB array. The OIB array is defined as all OIB except for the extreme HIMU basalts. Second, the correlation between Hf and Nd isotopic compositions of the OIB array as well as the slope of the array indicates that most of the Lu/Hf and Sm/Nd fractionations producing the array are coupled. The additional analyses did not change the slope of the OIB array $2\epsilon_{\text{Hf}} = 1\epsilon_{\text{Nd}}$. Third, as noted previously (Patchett, 1983b; Salters and Hart, 1991), the Hf isotope variation in MORB represents 45% of the global variation in oceanic basalts, while the Nd isotope variations in MORB represent only 22% of the total variation. The range in $^{176}\text{Hf}/^{177}\text{Hf}$ in MORB for a given $^{143}\text{Nd}/^{144}\text{Nd}$ is also close to the 45% of the total variation and clearly in MORB the Hf and Nd isotope variations are decoupled.

2.1. HIMU and recycling of oceanic crust

Several researchers have argued, mainly based on the Pb-isotope characteristics of the HIMU basalts, that this endmember represents a recycled oceanic crust component (Hofmann and White, 1980, 1982; Zindler et al., 1982). The Hf–Nd isotope variations are also consistent with HIMU basalts being derived from recycled oceanic crust. The HIMU basalts fall below the array formed by non-HIMU OIB basalts as the $^{176}\text{Hf}/^{177}\text{Hf}$ is lower for given $^{143}\text{Nd}/^{144}\text{Nd}$. These lower $^{176}\text{Hf}/^{177}\text{Hf}$ values indicate that, referenced against other OIB, Lu/Hf ratio of HIMU basalt source was low compared to the Sm/Nd ratio for some period of time. Fig. 2 shows the Hf and Nd isotope characteristics of a average N-type mid-ocean ridge basalt (MORB) (Hofmann, 1988) as a function of age of the basalt as well as age of the MORB source. It has been shown that both the Lu/Hf and the Sm/Nd ratios of MORBs are independent of Mg# and thus it can be assumed that these trace element ratios are representative for average unaltered N-type MORB oceanic crust (Salters, 1989). In addition, Staudigel et al. (1995) have shown that alteration has no real effect on the REE concen-

Table 1

Hf, Nd and Pb isotope data for MORB and OIB

	$^{176}\text{Hf}/^{177}\text{Hf}^a$	$^{143}\text{Nd}/^{144}\text{Nd}^b$	$^{206}\text{Pb}/^{204}\text{Pb}^c$	$^{207}\text{Pb}/^{204}\text{Pb}$	$^{208}\text{Pb}/^{204}\text{Pb}$
<i>Atlantic MORB</i>					
GS104 25-2	0.28325 \pm 7	0.513237	18.270	15.440	37.536
AD 3-3	0.28348 \pm 4	0.51329	17.784	15.605	38.298
GS 104 25-1	0.28310 \pm 5	0.513264	18.510	15.655	38.464
AD2-1	0.28309 \pm 4	0.513247	18.499	15.618	37.934
GS104 20-21	0.28319 \pm 4	0.513204	18.337	15.524	37.457
TR101 3D-9C	0.28341 \pm 5	0.513152	18.180	15.430	36.983
OC 180 9-2	0.28323 \pm 2	0.513203	18.317	15.441	37.575
OC 180 35-2	0.28330 \pm 4	0.513135	18.304	15.485	37.842
<i>Pacific MORB</i>					
1562.-1941	0.28317 \pm 2	0.513230	18.403	15.495	37.974
1565-1642	0.28334 \pm 1	0.513190	18.010	15.449	37.341
1567-1653	0.28325 \pm 4	0.513070	18.226	15.458	38.361
1559-1751	0.28322 \pm 3	0.513198	18.308	15.510	37.900
<i>Iceland</i>					
IT 3a	0.28318 \pm 5	0.51307	18.060	15.410	37.704
D 6	0.28320 \pm 3				
D2 (11)	0.28340 \pm 5	0.513158	18.197	15.401	37.741
Th 29	0.28336 \pm 4	0.513155	17.800	15.344	37.263
<i>Reykjanes</i>					
RE21	0.28325 \pm 3	0.512995	18.707	15.516	38.359
RE29	0.28324 \pm 2	0.513015			
RE 46	0.28340 \pm 3	0.513168	18.190	15.523	37.988
RE 56	0.28320 \pm 3	0.513032			
RE 100	0.28329 \pm 2	0.513083			
<i>Tubaii</i>					
TBA 22	0.28297 \pm 2	0.512904	20.956	15.756	40.234
TBA-B-3	0.28294 \pm 3	0.512914	21.115	15.746	40.343
<i>Rurutu</i>					
RRT B-30	0.28304 \pm 2	0.512925	20.050	15.656	38.804
RRT-B-19	0.28302 \pm 3	0.512928	20.338	15.679	39.800
<i>St. Helena</i>					
SH 76	0.28287 \pm 2	0.51286	20.566	15.745	39.916
SH209	0.28289 \pm 4	0.51285	20.780	15.769	40.069
SH18	0.28300 \pm 6	0.51287	20.839	15.772	40.098
SH34	0.28287 \pm 1	0.51276	20.805	15.777	40.096
SH194	0.28285 \pm 4	0.51282	20.584	15.764	39.930
SH 196	0.28287 \pm 1	0.51284	20.584	15.764	39.939
StH 2926	0.28283 \pm 4	0.512871	20.820	15.801	40.133
StH 2876	0.28288 \pm 3	0.512853			
StH 2882	0.28291 \pm 3	0.512857	20.896	15.791	40.131
StH 2893	0.28291 \pm 3	0.512843			
<i>Pitcairn</i>					
P3	0.28271 \pm 2	0.512502	17.782	15.477	38.872
P7	0.28278 \pm 2	0.512524	17.761	15.464	38.823
P9	0.28274 \pm 2	0.512545	17.795	15.475	38.844
P10	0.28265 \pm 1	0.512439	17.640	15.459	38.913
<i>Ascension</i>					
AS-1	0.28307 \pm 2				
AS#6	0.28303 \pm 2				
AS-3	0.28306 \pm 1				
AS-10	0.28302 \pm 1				

Table 1 (continued)

	$^{176}\text{Hf}/^{177}\text{Hf}^a$	$^{143}\text{Nd}/^{144}\text{Nd}^b$	$^{206}\text{Pb}/^{204}\text{Pb}^c$	$^{207}\text{Pb}/^{204}\text{Pb}$	$^{208}\text{Pb}/^{204}\text{Pb}$
<i>Crozet</i>					
CE13-1	0.28302	0.512865	18.892	15.583	39.034
CE9-1	0.28303	0.51284	18.846	15.572	38.984
CP30-3	0.28301	0.512856	18.930	15.588	39.913
<i>Kerguelen</i>					
KG6-2	0.28305 ± 6	0.512907	18.399	15.524	38.473
<i>New Amsterdam</i>					
NA14-2	0.28314 ± 3	0.512849	19.058	15.608	39.425
NA24-8	0.28314 ± 3	0.512886	19.113	15.603	39.470
NA27-8		0.51286	19.098	15.609	39.471
<i>St. Paul</i>					
SP1-5	0.28310 ± 3	0.512905	18.705	15.579	38.906
SP13-1	0.28306 ± 4	0.512853	18.701	15.573	38.875
<i>Comores</i>					
72-GC-1	0.28286 ± 4	0.512718	19.554	15.591	39.624
Ka77	0.28278 ± 3	0.512645	19.392	15.566	39.484
GC-33	0.28295 ± 2	0.512868	19.192	15.591	39.055
Mo 110	0.28295 ± 2	0.512832	19.339	15.602	39.197
AJ7-6	0.28294 ± 2	0.512888	20.216	15.654	39.917
<i>Rarotonga</i>					
866	0.28291 ± 2	0.512735	18.583	15.536	38.865
869	0.28297 ± 2	0.512676	18.310	15.511	38.704
<i>San Ambrosio and San Felix</i>					
99657	0.28289 ± 3	0.512724	18.972	15.570	38.903
99654	0.28285 ± 2	0.512621	18.956	15.555	38.860
99655	0.28276 ± 3	0.512562	19.250	15.593	39.231

Hf isotope data for most MORB, Iceland, Reykjanes, Tubaii, Rurutu, St. Helena (SH sample numbers), Pitcairn and Ascension are hot-SIMS data obtained using techniques described by Salters (1994). Hf and Nd data for the first six Atlantic MORB from Salters and Hart (1991); Pb data on these samples is new. All other Hf data were obtained at Cornell using thermal ionization mass spectrometry. Nd and Pb data for Iceland from Elliott et al. (1991), Reykjanes from Zindler et al. (1979), Pitcairn from Woodhead and McCulloch (1989). Nd and Pb data for Tubaii and Rurutu is unpublished data from Hauri and Hart (1993), Nd and Pb for the Pacific Ocean from Perfit, Nd-data for AD3-3 from O'Nions et al. (1977).

^a $^{176}\text{Hf}/^{177}\text{Hf}$ values corrected for fractionation using 0.6816 for $^{177}\text{Hf}/^{178}\text{Hf}$ and normalized to 0.282165 for JMC-475.

^b $^{143}\text{Nd}/^{144}\text{Nd}$ values normalized to 0.51264 for BCR-1.

^c Pb-isotope values corrected for fractionation using the values from Todt et al. (1996). Precision on Pb isotopes are 0.05% per amu.

trations of oceanic crust and it is assumed that the Lu/Hf ratios are also unaffected by alteration. The concentrations for the total oceanic crust will be lower than for MORB as approximately half of the oceanic crust is made up by cumulates and for elements like the REE and Hf the basaltic portion of the crust contains approximately 60% of the budget for those elements. The trajectories on Fig. 2 are for the composition of the endmember (recycled MORB or recycled oceanic crust); these can be determined from trace element ratios independent of absolute concentrations. The trajectory as a function of age of the endmember is relatively steep; the MORB-source has a higher Lu/Hf ratio than MORB as part of the

melting takes places in the presence of garnet (Salters and Hart, 1989) and the Lu/Hf of MORB is close to chondritic. This is not so much the case for Sm/Nd and $f_{(\text{Lu}/\text{Hf})}/f_{(\text{Sm}/\text{Nd})}$ (in a simple two stage model $f_{(\text{Lu}/\text{Hf})} = (\text{Lu}/\text{Hf})/(\text{Lu}/\text{Hf})_{\text{BSE}}$; (Salters and Hart, 1991)) is higher in the MORB source compared to MORB. These simple calculations show that 'pure' 1.7–1.4 Ga oceanic crust from a 2 Ga ago created MORB source or 2.1–1.8 Ga oceanic crust from a 3 Ga old MORB source can be the source for the Hf–Nd isotopic characteristics of the HIMU end-member. This is entirely consistent with the Pb-isotope characteristics of HIMU basalts which indicate an average age of 1.5–1.8 Ga. In addition, Fig. 2

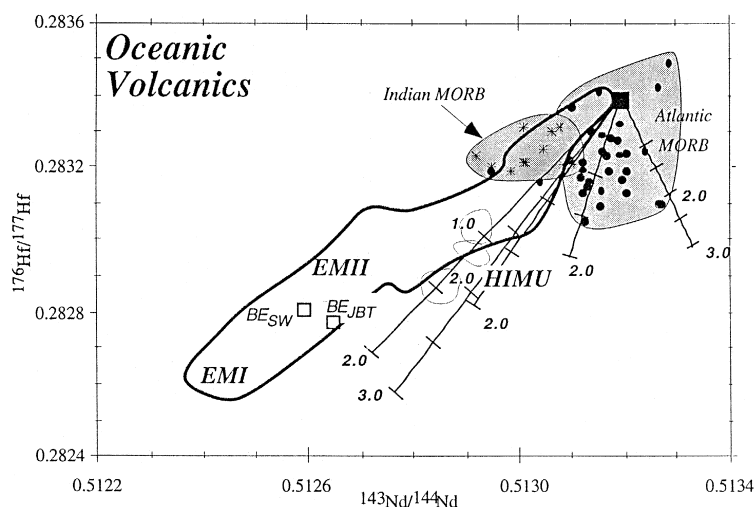


Fig. 2. Hf–Nd isotope correlation diagram showing the MORB and OIB field as well as the position of ancient MORB. Curves are the locations of present day isotope compositions of MORBs of different eruption ages from sources which are 2, or 3 Ga old. MORB composition with the shallowest slope evolution lines are 2.0 and 3.0 Ga old N-type MORB from Hofmann (1988). Numbers on the curves are the eruption ages of the basalts while the curves are for 2 and 3 Ga old MORB sources. The Hf and Nd isotopic composition of HIMU basalts can be produced by 1.4 to 2.1 Ga old MORB from a MORB source formed 2 to 3 Ga ago. MORB (oceanic crust) evolution curves for estimates of oceanic crust from Staudigel et al. (1995) are also shown. This estimate results in the two right most evolution lines on the diagram. The one remaining curve is the N-type MORB estimate of a 2 Ga old source from Sun and McDonough (1989). Symbols as in Fig. 1.

shows trajectories for the estimates of oceanic crustal compositions determined by Staudigel et al. (1995). Altered oceanic crust, ‘super’ composite (Staudigel et al., 1995), has, surprisingly, higher Sm/Nd as well as Lu/Hf (Hf calculated assuming chondritic Sm/Hf ratio) than the N-type MORB estimate of Hofmann (1988). Consequently, the ‘super’ composite results in higher $^{143}\text{Nd}/^{144}\text{Nd}$ values than Hofmann’s N-type MORB estimate. Thirdly, the trajectories for N-type MORB estimates from Sun and McDonough (1989) are shown. Their N-type MORB estimate is closer to Hofmann, although it also has a higher Sm/Nd ratio. Although the Hf–Nd isotope data show that the low $^{176}\text{Hf}/^{177}\text{Hf}$ values for HIMU basalts can be explained by a recycled oceanic crust component, the contribution of components other than recycled crust to HIMU is not well determined. If the recycled crust is similar to the estimate provided by Hofmann (1988), then HIMU can be pure oceanic crust. Other estimates with more depleted Sm/Nd and Lu/Hf ratios require the addition of an enriched component to achieve HIMU type compositions. Based on these simple calculations it can be concluded that although the origin of HIMU basalts

can be complex, it will most likely involve a large component of oceanic crust.

The formation of the oceanic crust also produces depleted oceanic lithosphere. The use of only oceanic crust to generate HIMU requires separation of depleted oceanic lithosphere from the basaltic crust. It has been shown that the Lu/Hf and Sm/Nd ratios of the depleted lithosphere are such that it will very quickly develop a unique isotopic signature (Salters and Zindler, 1995). This extreme isotopic signature of the residual lithosphere can potentially be a limit on the amount of oceanic crust that can be separated. However, the concentrations in the residual peridotitic lithosphere are so low that a large amount (in excess of 30%) would be required to generate significant shifts in the isotopic composition caused by simple mixing with residues from MORB melting (see Fig. 3). The slope of the mixing array of bulk earth with 2 Ga old oceanic lithosphere is almost parallel to the OIB array.

Although MORBs are often viewed as being derived from a relatively homogeneous reservoir, MORBs represent a large range of the global variation in both the Hf and Pb isotopic composition of

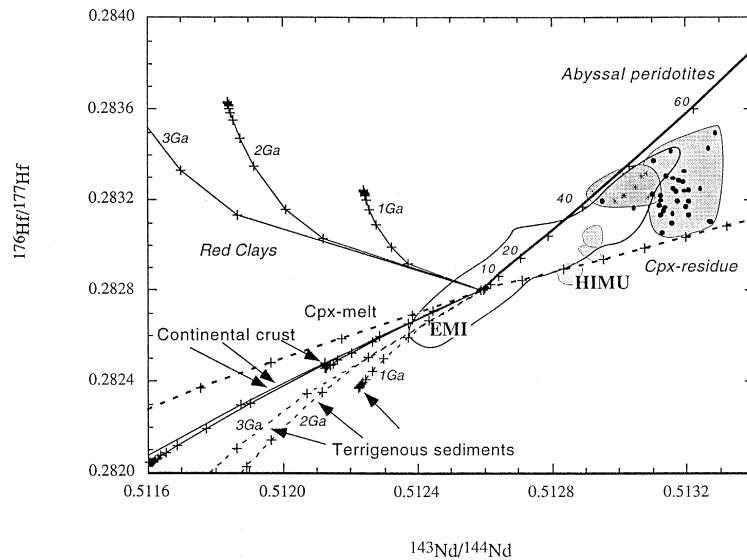


Fig. 3. Hf–Nd isotope correlation diagram showing mixing curves between the center of the OIB array and materials that have previously been proposed as components that exist in the mantle and can potentially produce some of the isotopic variations observed in basalts. Tick marks on mixing curves are at 1, 2, 5, 10, 20, 30, 40, 50, 60, 70, 80, 90 and 100% addition of the endmember to BE_{SW} . Continental crust estimate from Rudnick and Fountain (1995). Crustal composition based on the average of Precambrian granite data (Vervoort and Patchett, 1996; Vervoort et al., 1996a) is similar to the estimate of Rudnick and Fountain. Terrigenous sediment and red clay data from (Ben Othman et al., 1984; Patchett et al., 1984; White et al., 1986). Melt and residue calculated with clinopyroxene as the mineral controlling the trace element fractionation used partition coefficients of Hart and Dunn (1992). The curve for the cpx melts and residues represents the locus of melts (or residues) resulting from 2% melting of BE as a function of age. Tick marks on curves indicate 500 Ma age increments. Mixing curve for abyssal peridotites uses an estimate of average abyssal peridotite based on data of (Johnson et al., 1990; Johnson and Dick, 1992).

oceanic volcanics (45% and 65%, respectively). Fig. 4 displays the Hf–Pb isotope variations in an effort to determine whether the large range in Hf-isotopes in MORB is correlated to the Pb-isotopes. Fig. 4 shows, however, that the MORB field on the Pb–Hf isotope correlation diagram shows a trend internal to the OIB field and that the processes that result in the Pb–Hf variations in MORB are not associated with HIMU type characteristics or processes that result in HIMU like recycling of oceanic crust internal to DMM (depleted MORB mantle).

3. The bulk earth value and the MORB-field

In a recent paper Blichert-Toft and Albarède (1997) reported that the chondritic earth has $^{176}\text{Hf}/^{177}\text{Hf}$ values that make it plot at the edge of the OIB array on a Hf–Nd isotope correlation diagram. Their data displays a limited range in $^{176}\text{Hf}/^{177}\text{Hf}$ and the individual $^{176}\text{Hf}/^{177}\text{Hf}$ values

do not correlate with the rather large range in Lu/Hf values for these chondrites. This lack of correlation between the parent-daughter ratios and the isotope ratios resulted in the weighted average of 25 chondrites (C, E and O chondrites) as the choice for bulk earth. Because only one chondrite has been characterized for both Hf and Nd isotopes a direct comparison of the Nd and Hf isotope variations is not possible. However, when grouped by meteorite class the Hf and Nd isotope variations in chondrites can be compared and are shown to be negatively correlated (correlation coefficient, $R^2 = 0.76$, see Fig. 5). In addition, the $^{176}\text{Lu}/^{177}\text{Hf}$ and $^{147}\text{Sm}/^{144}\text{Nd}$ ratios of the grouped chondrites are also correlated ($R^2 = 0.98$) as well as $^{147}\text{Sm}/^{144}\text{Nd}$ and $^{143}\text{Nd}/^{144}\text{Nd}$. Grouped by class the Lu/Hf and $^{176}\text{Hf}/^{177}\text{Hf}$ of the chondrites show the poorest correlation. This correlated variation in chondrite compositions allows us to choose a chondritic bulk earth that lies in the center of the OIB array, instead of being positioned at an extreme edge. BE would lie on the intersection

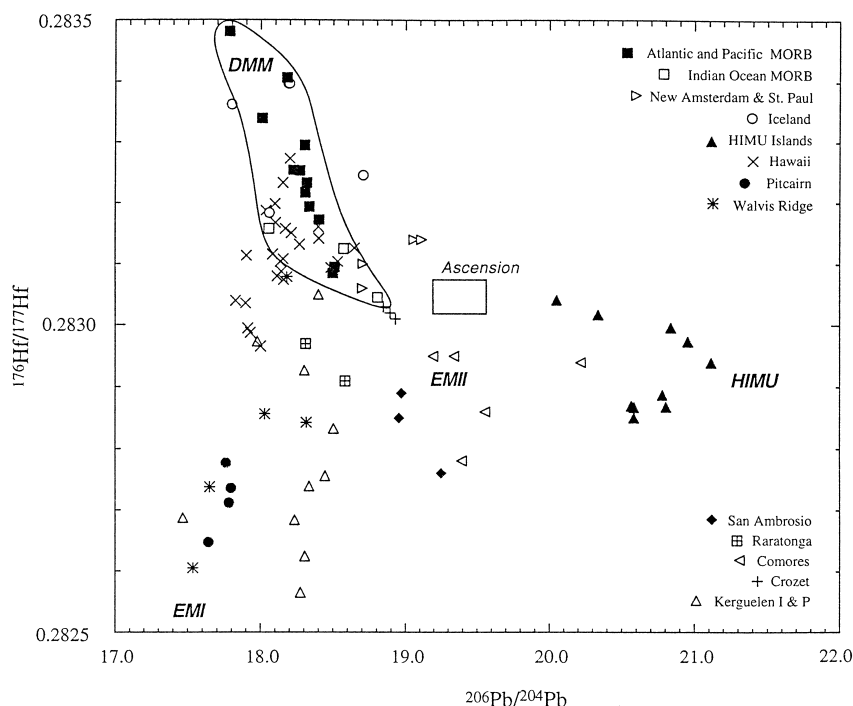


Fig. 4. Hf–Pb isotopic variations of oceanic basalts showing that MORB mix internal to the OIB field and do not mix with a HIMU component. This feature is also observed on a Nd–Hf isotope correlation diagram. In addition to the data in the table unpublished data of Meen are plotted for Mid-Cayman Rise MORB. Field for Ascension island is derived using the Pb-isotope data reported by Weis (1983).

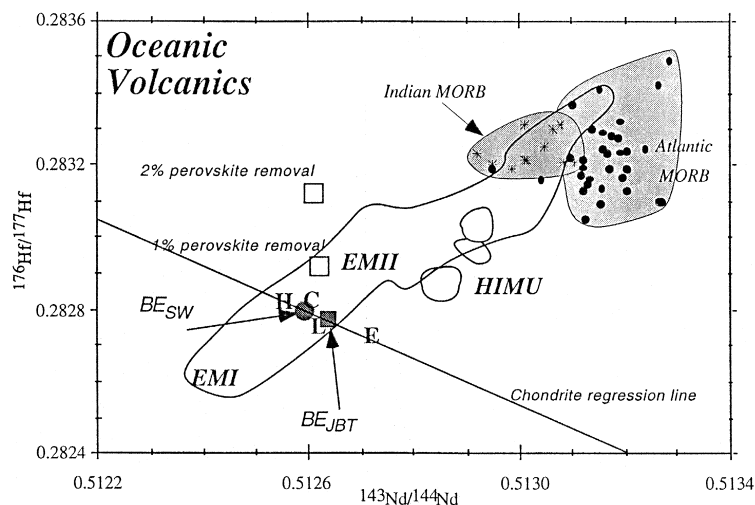


Fig. 5. Hf–Nd isotope diagram showing the effect of removal of different amounts of perovskite on the composition of the silicate earth. The squares indicate where the 'residual' silicate earth would plot after removal of 1 or 2% of perovskite. This model assumes removal and isolation of perovskite at least 4.0 Ga ago. Clearly 1% perovskite removal can explain the shift of the OIB array to high $^{176}\text{Hf}/^{177}\text{Hf}$ values. Chondritic earth value from (Blichert-Toft and Albarède, 1997). Perovskite partition coefficients $D_{\text{Hf}} = 9.0$, $D_{\text{Lu}} = 1.2$, $D_{\text{Sm}} = 0.3$ and $D_{\text{Nd}} = 0.15$ are derived from the studies of Kato et al. (Kato et al., 1988a,b). Bold letters near the chondrite regression line represent the average for the different classes of meteorites: C = carbonaceous, E = enstatite, H = ordinary high Fe and L = ordinary low Fe. Data for Sm–Nd systematics of the chondrites are from (Jacobsen and Wasserburg, 1980, 1984 and DePaolo et al., 1991).

of the chondritic array with the oceanic basalt array (see Fig. 5). This new estimate results in a change in both the Hf and Nd isotope value of bulk earth (BE). The Nd-isotope composition of BE was determined rather arbitrary and chosen to be close to the mode of the $^{147}\text{Sm}/^{144}\text{Nd}$ values of chondrites (Jacobsen and Wasserburg, 1980, 1984). The Nd–Hf isotope correlation of chondrite and the proposed change in Be parent–daughter ratios is less than 1%. With BE at the intersection of the OIB and chondrite array the present day isotope ratios for BE would be 0.2828 and 0.51259 for $^{176}\text{Hf}/^{177}\text{Hf}$ and $^{143}\text{Nd}/^{144}\text{Nd}$ respectively and the associated parent–daughter ratios would be 0.0335 for $^{176}\text{Lu}/^{177}\text{Hf}$ and 0.1952 for $^{147}\text{Sm}/^{144}\text{Nd}$. The isotopic composition of the ‘new’ BE would be closer to C-chondrites than the previous estimates and is named BE_{SW} indicating the Salters and White estimate.

Before any changes are made in the BE $^{143}\text{Nd}/^{144}\text{Nd}$ value it should be understood that relatively few E- and O-chondrites have been analyzed for Nd-isotopic composition (Jacobsen and Wasserburg, 1980, 1984; DePaolo et al., 1991). and therefore the slope of the line has a large uncertainty. The anti-correlation observed in Fig. 5 needs to be supported by additional Nd-isotope data on E- and O-type chondrites before confident changes are made in Be $^{143}\text{Nd}/^{144}\text{Nd}$ and $^{176}\text{Hf}/^{177}\text{Hf}$. Jacobsen and Wasserburg (1984) noted that there was no good explanation for the range they found in $^{143}\text{Nd}/^{144}\text{Nd}$ and Sm/Nd and concluded that these are small scale heterogeneities. The addition of the Hf-isotopes suggest that the small scale heterogeneities persist for other isotope systems as well and, in addition, it suggests that these heterogeneities are correlated. At present we consider both compositions BE_{JBT} and BE_{SW} are equally viable.

The exact composition of BE has important consequences for the evolution of the Earth’s mantle. Only some Kerguelen basalts have Hf and Nd isotope ratios similar to BE_{JBT} , but these basalts have Sr isotope ratios too different to be considered BE. The BE_{JBT} location suggests that present-day OIB do not sample primitive mantle (Blichert-Toft and Albarède, 1997). Furthermore, the Hf–Nd characteristics of OIB indicates that over time the Earth’s mantle has experienced a higher Lu/Hf than BE_{JBT} . As none of the OIB data trends towards the chon-

dritic earth it can be assumed that all OIB sources are offset to higher time-integrated Lu/Hf (resulting in higher present-day $^{176}\text{Hf}/^{177}\text{Hf}$) for a given Sm/Nd value. Blichert-Toft and Albarède (1997) explain the offset of the OIB array by a presence of basalt in the Earth’s mantle, which is not sampled. Displacement of the array requires that garnet is a residual phase in basalt genesis. Only with garnet residual present, will the resulting basalts have large enough Lu/Hf fractionations to cause a significant shift in $^{176}\text{Hf}/^{177}\text{Hf}$ of the OIB array. This can be seen in the evolution curves for oceanic crust and MORB in Fig. 2 which are all associated with larger variations in $^{176}\text{Hf}/^{177}\text{Hf}$ than in $^{143}\text{Nd}/^{144}\text{Nd}$. Garnet plays an important role in the genesis of MORB (Salters and Hart, 1989; Johnson et al., 1990). If the isolated basalts are MORB-like in composition, 2 to 4% of the mass of the mantle has to be kept isolated depending on the age of the basalts (3 to 2 Ga respectively). Although the basalts are left unsampled, the melt residue of these basalts, will have characteristics akin to abyssal peridotites, and has to mix back into the mantle. Assuming the basalts formed by 10% melting, nine times as much residue has to be recycled in the mantle resulting in 18 to 36% of the total mass of the mantle being residue that is mixed back. Fig. 3 shows that mixing of mantle with 2 Ga old depleted peridotite (similar to average abyssal peridotite) results in an array that fits the upper part of the OIB array.

Another scenario that can explain the shift of the OIB array to higher $^{176}\text{Hf}/^{177}\text{Hf}$ compared to the chondrite value of Blichert-Toft and Albarède (1997; BE_{JBT}) is fractionation of Mg-perovskite during the early stages of the Earth’s history. Blichert-Toft and Albarède (1997) discuss the role of perovskite in explaining the variation within the OIB and MORB field and show that melting with perovskite as a residual phase cannot explain the variations within the OIB and MORB field. It has been proposed that a magma ocean existed during the early history of the Earth and that perovskite crystallization from this magma ocean resulted in an upper mantle that is differs from C1 chondrite (Agee and Walker, 1988). Previously, the fact that the chondritic earth was positioned within the OIB array was one of the strongest arguments against the existence of a magma ocean and possible fractionation perovskite from of

the silicate earth. The composition BE_{sw} will continue to be a strong argument against fractionation of perovskite from a magma ocean. Hf is compatible in perovskite and crystallization and isolation of only small amounts of perovskite is required to change the Lu/Hf in the remaining magma significantly (2% Lu/Hf change for 1% perovskite crystallization) without a significant change (0.2% change for 1% perovskite fractionation) in the Sm/Nd of the remaining magma. Fig. 5 shows that isolation of 1% perovskite shortly after the accretion of the planet and the formation of the core (between 4.4 and 3.8 Ga ago) already results in a shift in the $^{176}\text{Hf}/^{177}\text{Hf}$ of the remaining bulk silicate earth and will move the BSE value up by approximately 3 ϵ units. The BSE remaining after perovskite removal is thus internal to the OIB field.

A constraining factor on the amount of perovskite fractionation is the Earth's Sm/Zr and Sm/Hf ratio. The chondritic Sm/Hf ratio is 1.38 (Sm/Zr = 0.036), while the Sm/Hf of the remaining BSE (after 1% perovskite fractionation) would be 1.47 (Sm/Zr = 0.038). These values are within the error limits of our best estimates of the BSE, which could tolerate up to 2% perovskite fractionation (Hart and Zindler, 1986; McDonough and Sun, 1995). Salters and Zindler (1995) have argued based on the Sm/Hf and Sm/Zr ratios of abyssal peridotites as well as basalts that part of the mantle has Sm/Zr and Sm/Hf ratios higher than chondritic values (superchondritic). The positioning of the chondritic earth at the edge of the OIB-array seems confirmation of the existence of these superchondritic values. It thus seems entirely feasible that perovskite fractionation during the early stages of the Earth's history, followed by isolation of a small amount of perovskite during the history of the earth can explain the more radiogenic Hf isotopic composition of OIB array as compared to the chondritic earth.

Perovskite, isolated for more than 4 Ga, will have extreme isotopic compositions. The partition coefficients (Kato et al., 1988a,b) are such that the perovskite will have radiogenic $^{143}\text{Nd}/^{144}\text{Nd}$ combined with unradiogenic $^{176}\text{Hf}/^{177}\text{Hf}$ as the ingrowth of ^{176}Hf is retarded due to the low Lu/Hf ratios in the perovskite ($^{176}\text{Hf}/^{177}\text{Hf} = 0.2802$ and $^{143}\text{Nd}/^{144}\text{Nd} = 0.5185$ for 4.4 Ga old perovskite, Lu/Hf = 0.0319, and Sm/Nd = 0.6485). The Nd/Hf ratio of

perovskite is low and mixing of ancient perovskite with mantle materials will result in a decoupling of the Hf–Nd isotope systematics as mixing lines will show extreme curvature. The mixing back into the mantle of ancient perovskite will change the Hf-isotopic composition before any effects on the Nd-isotopic composition can be observed.

MORB show a decoupling of the Hf and Nd isotope systems as almost the complete range in $^{176}\text{Hf}/^{177}\text{Hf}$ exists at constant $^{143}\text{Nd}/^{144}\text{Nd}$ (see Fig. 2). This decoupling of the Hf from the Nd isotopes has required rather arbitrary models that were not supported by other evidence (Salters and Hart, 1991; Salters and Zindler, 1995; Blichert-Toft and Albarède, 1997). For example, if MORB are the residue of a single depletion event than a fortuitous trade off between degree of melting and the amount of residual garnet is required to explain the large range in $^{176}\text{Hf}/^{177}\text{Hf}$ for constant $^{143}\text{Nd}/^{144}\text{Nd}$ (Salters and Hart, 1991). Alternatively, the low $^{176}\text{Hf}/^{177}\text{Hf}$ end of the MORB field can be the residue from melting in the absence of garnet (clinopyroxene controlling the trace element fractionations (Blichert-Toft and Albarède, 1997), but no such melts are observed at the Earth's surface. A role for perovskite has been suggested to explain the decoupling of Hf and Nd-isotopes, but these models are also ad-hoc (Salters and Hart, 1991; Salters and Zindler, 1995). The suggested presence of ancient perovskite in the mantle can also provide the explanation for the shape of the MORB field as the addition of up to 1% of perovskite can explain the total range in Hf isotopic composition and the decoupling of the Hf from the Nd isotopes. It is therefore most likely that the decoupling of the Hf and Nd isotopes in MORB is the result of pollution of the MORB reservoir with small (up to 1%) amounts of perovskite. Our explanation for the MORB-field is different than the explanation of Blichert-Toft and Albarède (1997) who find no role for perovskite in explaining the Hf–Nd variations in the MORB and OIB field. The main difference between our calculations and Blichert-Toft and Albarède (1997) is the partition coefficients used for perovskite. We agree with Blichert-Toft and Albarède (1997) that the variation within the OIB field excludes a role for perovskite. However, with our choice of partition coefficients for perovskite, the Lu/Hf fractionation in

the residual perovskite is extreme (factor of 8 change compared to BE) while the Sm/Nd fractionation is less (factor of 2). This partition coefficients are well within the range reported by (Kato et al., 1988a,b) but the fractionation is more extreme than calculated by Blichert-Toft and Albarède (1997). This more extreme fractionation for Lu/Hf allows the MORB field to be explained by mixing with ancient perovskite isolated since crystallization from a magma ocean.

An unsatisfying aspect of the long term isolation of both basalt and perovskite is that there is no mantle process that can account for this isolation. The small amount of perovskite required makes it easier to 'hide' but no real answer is available for either scenario.

4. The slope of the OIB array

The good correlation between the Hf and Nd-isotopes in OIB sources is best explained by time integrated Lu/Hf and Sm/Nd fractionations which are correlated. The slope of the array represents information on the time integrated $f_{(Lu/Hf)}/f_{(Sm/Nd)}$ (Patchett, 1983b; Salters and Hart, 1991; Beard and Johnson, 1993). There have been several suggestions on the source materials for the enriched mantle components (EMI and EMII; (Zindler and Hart, 1986; Hart, 1988; Hart and Staudigel, 1989; Weaver, 1991) as examples). The addition of a recycled oceanic or deep-sea sediment component has often been invoked for the EMI endmember and the addition of a continental component has often been asserted for the EMII endmember.

Fig. 3 shows potential mixing curves of basalts sources within the OIB array with different types of sediment as well as with average continental crust (Rudnick and Fountain, 1995). Mixing curves of the recycled materials and a MORB-type source (DMM) instead of an BE-type source have shallower slopes as the Hf/Nd ratio in a MORB source is higher. The mixing curves of sediments with DMM lie even further of the OIB array than the mixing arrays shown in Fig. 3. Except for 1 Ga old terrigenous sediments, mixing of just one of the potentially recycled material (sediment or crust) with material from within the mantle array cannot explain the

observed slope of the OIB array. Thus if any of those potentially recycled components is part of any of the OIB sources than it has to be mixed with the ambient mantle thoroughly and at constant ratio before it is sampled at the Earth's surface. For example, if red clays are part of the EMI source than the amount of red clay that is part of the EMI source has to be relatively constant at every location where EMI is sampled. Less than 0.5% of red clay can be tolerated in any of the basalt sources that lie in the OIB array. However, the mixing arrays are such that red clays alone cannot produce the low $^{176}\text{Hf}/^{177}\text{Hf}$ that is observed in the EMI basalts. The shallow slopes of most of the sediments indicates that a component with a larger Lu/Hf fractionation (without a significant change in the Sm/Nd fractionation) is required to 'steepen' the array. Fig. 2 shows that oceanic crust is clearly a candidate for the component with the larger Lu/Hf fractionation. But again, a rather constant ratio of sediment and igneous oceanic crust is required to produce the tight OIB array.

The mixing curves of bulk earth with continental crust and with most sediments are all less steep than the OIB array (except for 1 Ga old sediments), thus there has to be another component or process with a larger relative Lu/Hf fractionation as compared to Sm/Nd fractionations (higher $f_{(Lu/Hf)}/f_{(Sm/Nd)}$ values). The processes that can explain the steep slope of the OIB array involves enrichment and depletion processes that are associated with melting. Shallow level melting, whereby the fractionation of Lu/Hf and Sm/Nd is controlled by clinopyroxene results in too low $f_{(Lu/Hf)}/f_{(Sm/Nd)}$ values (see Fig. 3; Salters and Hart, 1991). Garnet and amphibole are the two most obvious phases that can effect $f_{(Lu/Hf)}/f_{(Sm/Nd)}$ different than clinopyroxene. Although amphibole does fractionate Lu/Hf more than clinopyroxene, there is a concomitant change in Sm/Nd fractionation (Salters and Hart, 1991) and the net result is not large enough to explain the slope of the OIB array. Garnet on the other hand is clearly able to fractionate Lu/Hf ratio more significantly and melting in the presence of garnet will result in higher $f_{(Lu/Hf)}/f_{(Sm/Nd)}$ values. Just modest amounts of garnet (modal garnet-cpx ratios of 0.15–0.25) are required to result in the appropriate $f_{(Lu/Hf)}/f_{(Sm/Nd)}$ values and will explain the slope of the OIB array. An example of that is seen in the mixing curve of

BE_{SW} with 2 Ga old abyssal peridotite. Abyssal peridotites are the residues of melting that took partly place in the garnet stability field (Johnson et al., 1990). It therefore seems very likely that the high end of the OIB array (higher $^{143}\text{Nd}/^{144}\text{Nd}$ and $^{176}\text{Hf}/^{177}\text{Hf}$ than BE) is formed of melt residues that involved garnet.

Alternatively, the low end of the OIB array can also be explained by the recycling of a fixed mixture of sediment and ancient basalt (MORB for example) with BE. As shown for the HIMU endmember, mixing with ancient MORB produces an array with a steeper slope than the OIB field. Again, ancient red clay is not a potential endmember candidate as its isotopic composition is too extreme. However, mixtures of ancient MORB (2 to 3 Ga) with continental crust or continentally derived sediments could produce sources that would fall in the OIB field. For example, the low $^{176}\text{Hf}/^{177}\text{Hf}$ – $^{143}\text{Nd}/^{144}\text{Nd}$ end of the OIB field can be reached by a 70:30 mixture of 2.2 Ga old MORB with 2.2 Ga old continental crust. More ancient sources would produce material that falls in the extension of the OIB array at lower $^{143}\text{Nd}/^{144}\text{Nd}$ and $^{176}\text{Hf}/^{177}\text{Hf}$ values. Less than 15% continental crust, or more than 30% would result in mixture with slopes different than the OIB array. The mixing models that involve either sediments or continental crust have the disadvantage that they will not be able to produce the Ce/Pb and Nb/U characteristics of OIB which are so different from both sediments and BE. These numbers are to illustrate the type of constraints the OIB array provides and should be used if a certain origin for the endmembers of the OIB array is preferred. These above models are illustrative and highly non-unique and thus provide boundary conditions that have to be taken into account by the various models. However, the models have in common that during a process requiring fractionation (melting) in the presence of garnet, and that recycling of continental crust and sediments can only explain a limited part of the OIB array.

5. Conclusions

Further research is required to determine the composition of the bulk silicate earth (BSE) in Hf–Nd isotope space. The location of BSE is critical in

evaluating the existence of a magma ocean during the early history of the Earth. BSE can be internal to the OIB array if BSE is determined by the intersection of the OIB array and the meteorite array and no magma ocean is required. If BSE is located below the OIB array a ‘hidden’ component is needed to explain why BSE is external to the OIB field. Two scenarios for the hidden component are possible. In one scenario this hidden component is basalt Blichert-Toft and Albarède (1997) and again no magma ocean is required. In the second scenario this ‘hidden’ component is perovskite and the existence of a magma ocean is suggested. In addition, fractionation and isolation of perovskite from this magma ocean results in a shift in isotopic composition of the residual magma as well as the development of extreme isotopic signatures in the isolated perovskite. Pollution of the MORB reservoir with small amounts of this extreme perovskite composition can explain the decoupling between the Hf and Nd isotopes in MORB.

Except for the HIMU endmember, the Hf and Nd-isotopic composition in OIB are extremely well correlated. This correlation can only be explained, if a significant part of the fractionation that resulted in the isotopic variability is melting in the presence of garnet. Mixing of continental crust alone, sediments alone, or sediment–continental crust mixtures cannot explain the correlated variation in Hf and Nd isotopes in OIB. The Hf and Nd isotopic compositions of the HIMU endmember are consistent with the presence of significant amount of recycled oceanic crust in this endmember.

Acknowledgements

Stan Hart, Jon Patchett, Rick Carlson and Roy Odom are thanked for their constructive criticisms on the paper. This work is supported by NSF grant EAR95-26609 to VS.

References

- Agee, C.B., Walker, D., 1988. Mass balance and phase density constraints on early differentiation of chondritic mantle. *Earth Planet. Sci. Lett.* 90, 144–156.
- Beard, B.L., Johnson, C.M., 1993. Hf isotope composition of late Cenozoic basaltic rocks from northwestern Colorado, USA:

- New constraints on mantle enrichment processes. *Earth Planet. Sci. Lett.* 119, 495–509.
- Ben Othman, D., Fourcade, S., Allègre, C.J., 1984. Recycling processes in granite granodiorite complex genesis. The Querigut case studied by Nd–Sr isotope systematics. *Earth Planet. Sci. Lett.* 69, 290–300.
- Ben Othman, D., White, W.M., Patchett, J., 1989. The geochemistry of marine sediments, island arc magma genesis, and crust–mantle recycling. *Earth Planet. Sci. Lett.* 94, 1–21.
- Blichert-Toft, J., Albarède, F., 1997. The Lu–Hf isotope geochemistry of chondrites and the evolution of the mantle–crust system. *Earth Planet. Sci. Lett.* 148, 243–258.
- DePaolo, D.J., Linn, A.M., Schubert, G., 1991. The continental crustal age distribution: Methods of determining mantle separation ages from Sm–Nd isotopic data and application to the southwestern United States. *J. Geophys. Res.* 96, 2071–2088.
- Elliott, T.R., Hawkesworth, C.J., Gronvold, K., 1991. Dynamic melting of the Iceland plume. *Nature* 351, 201–206.
- Hart, S.R., 1988. Heterogeneous mantle domains: signatures, genesis and mixing chronologies. *Earth Planet. Sci. Lett.* 90, 273–296.
- Hart, S.R., Dunn, T., 1992. Experimental cpx/melt partitioning of 23 trace elements. *Contrib. Min. Petrol.* 113, 1–18.
- Hart, S.R., Gerlach, D.C., White, W.M., 1986. A possible new Sr–Nd–Pb mantle array and consequences for mantle mixing. *Geochim. Cosmochim. Acta* 50, 1551–1557.
- Hart, S.R., Staudigel, H., 1989. Isotopic characterization and identification of recycled components. Crust/mantle recycling at convergence zones.
- Hart, S.R., Zindler, A., 1986. In search for bulk-earth composition. *Chem. Geol.* 57, 247–267.
- Hauri, E.H., Hart, S.R., 1993. Re–Os isotope systematics of HIMU and EMII oceanic island basalts from the South Pacific Ocean. *Earth Planet. Sci. Lett.*
- Hofmann, A.W., 1988. Chemical differentiation of the Earth: the relationship between mantle, continental crust and oceanic crust. *Earth Planet. Sci. Lett.* 90, 297–314.
- Hofmann, A.W., White, W.M., 1980. The role of subducted oceanic crust in mantle evolution. *Carnegie Inst. Wash. Yearb* 79, 477–483.
- Hofmann, A.W., White, W.M., 1982. Mantle plumes from ancient oceanic crust. *Earth Planet. Sci. Lett.* 57, 421–436.
- Jacobsen, S.B., Wasserburg, G.J., 1980. Sm–Nd isotopic evolution of chondrites. *Earth Planet. Sci. Lett.* 50, 139–155.
- Jacobsen, S.B., Wasserburg, G.J., 1984. Sm–Nd isotopic evolution of chondrites and achondrites, II. *Earth Planet. Sci. Lett.* 67, 137–150.
- Johnson, K.T.M., Dick, H.J.B., 1992. Open system melting and temporal and spatial variation of peridotite and basalt at the Atlantis II fracture zone. *J. Geophys. Res.* 97, 9219–9241.
- Johnson, K.T.M., Dick, H.J.B., Shimizu, N., 1990. Melting in the oceanic upper mantle: an ion microprobe study of diopsides in abyssal peridotites. *J. Geophys. Res.* 95, 2661–2678.
- Kato, T., Ringwood, A.E., Irifune, T., 1988a. Constraints on element partition coefficients between MgSiO_3 perovskite and liquid determined by direct measurements. *Earth Planet. Sci. Lett.* 90, 65–68.
- Kato, T., Ringwood, A.E., Irifune, T., 1988b. Experimental determination of element partitioning between silicate perovskites, garnets and liquids: constraints on early differentiation of the mantle. *Earth Planet. Sci. Lett.* 89, 123–145.
- McDonough, W.F., Sun, S.-S., 1995. The composition of the Earth. *Chem. Geol.* 120, 223–253.
- O’Nions, R.K., Hamilton, P.J., Evensen, N.M., 1977. Variations in $^{143}\text{Nd}/^{144}\text{Nd}$ and $^{87}\text{Sr}/^{86}\text{Sr}$ ratios in oceanic basalts. *Earth Planet. Sci. Lett.* 34, 13–22.
- Patchett, P.J., 1983a. Hafnium isotope results from mid-ocean ridges and Kerguelen. *Lithos* 16, 47–51.
- Patchett, P.J., 1983b. Importance of the Lu–Hf isotopic system in studies of planetary chronology and chemical evolution. *Geochim. Cosmochim. Acta* 47, 81–91.
- Patchett, P.J., Kouvo, O., Hedge, C.E., Tatsumoto, M., 1981. Evolution of continental crust and mantle heterogeneity: evidence from Hf isotopes. *Contrib. Min. Petrol.* 78, 279–297.
- Patchett, P.J., Tatsumoto, M., 1981a. The hafnium isotopic evolution of lunar basalts. *Lunar Planet. Sci.* 12, 819–821.
- Patchett, P.J., Tatsumoto, M., 1980. Hafnium isotope variations in oceanic basalts. *Geophys. Res. Lett.* 7, 1077–1080.
- Patchett, P.J., Tatsumoto, M., 1981b. Lu/Hf in chondrites and definition of a chondritic hafnium growth curve. *Lunar Planet. Sci.* 12, 822–824.
- Patchett, P.J., White, W.M., Feldmann, H., Kielinczuk, S., Hofmann, A.W., 1984. Hafnium/rare earth element fractionation in the sedimentary system and crustal recycling into the Earth’s mantle. *Earth Planet. Sci. Lett.* 69, 365–378.
- Rudnick, R.L., Fountain, D.M., 1995. Nature and composition of the continental crust: a lower crustal perspective. *Rev. Geophys.* 33, 267–309.
- Salters, V.J.M., 1989. The use of Hf-isotopes and High Field Strength Elements to constrain magmatic processes and magma sources. PhD, Thesis, Massachusetts Institute of Technology.
- Salters, V.J.M., 1994. $^{176}\text{Hf}/^{177}\text{Hf}$ determination in small samples by a high temperature SIMS technique. *Anal. Chem.* 66, 4186–4189.
- Salters, V.J.M., 1996. The generation of mid-ocean ridge basalts from the Hf and Nd isotope perspective. *Earth Planet. Sci. Lett.* 141, 109–123.
- Salters, V.J.M., Hart, S.R., 1989. The Hf-paradox and the role of garnet in the MORB source. *Nature* 342, 420–422.
- Salters, V.J.M., Hart, S.R., 1991. The mantle sources of ocean islands and arc basalts: the Hf isotope connection. *Earth Planet. Sci. Lett.* 104, 364–380.
- Salters, V.J.M., Zindler, A., 1995. Extreme $^{176}\text{Hf}/^{177}\text{Hf}$ in the sub-oceanic mantle. *Earth Planet. Sci. Lett.* 129, 13–30.
- Shirey, S.B., Hanson, G.N., 1986. Mantle heterogeneity and crustal recycling in Archean granite–greenstone belts: evidence from Nd isotopes and trace elements in the Rainy Lake area, Superior Province, Ontario, Canada. *Geochim. Cosmochim. Acta* 50, 2631–2651.
- Staudigel, H., Davies, G.R., Hart, S.R., Marchant, K.M., Smith, B.M., 1995. Large scale isotopic Sr, Nd and O isotopic anatomy of altered oceanic crust: DSDP/ODP sites 417/418. *Earth Planet. Sci. Lett.* 130, 169–185.
- Stille, P., Unruh, D.M., Tatsumoto, M., 1983. Pb, Sr, Nd and Hf

- isotopic evidence of multiple sources for Oahu, Hawaii basalts. *Nature* 304, 25–29.
- Stille, P., Unruh, D.M., Tatsumoto, M., 1986. Pb, Sr, Nd and Hf isotopic constraints on the origin of Hawaiian basalts and evidence for a unique mantle source. *Geochim. Cosmochim. Acta* 50, 2303–2319.
- Sun, S.-S., McDonough, W.F., 1989. Chemical and isotopic systematics of oceanic basalts: implications for mantle composition and processes. In: Saunders, A.D., Norry, M.J., (Eds.), *Magmatism in the Ocean Basins*, vol. 42 Geological Society, pp. 313–345.
- Tatsumoto, M., Unruh, D.M., Patchett, P., 1981. U–Pb and Lu–Hf systematics of Antarctic meteorites. *Mem. Nat. Inst. Polar. Res. Tokyo, Spec. Issue* 20, 237–249.
- Todt, W., Cliff, R.A., Hanserr, A., Hofmann, A.W., 1996. Evaluation of a ^{202}Pb – ^{205}Pb double spike for high-precision lead isotope analysis. In: Basu, S.H.A.A., (Ed.), *Earth Processes, Reading the Isotope record*, AGU.
- Vervoort, J.D., Patchett, P.J., 1996. Behavior of hafnium and neodymium isotopes in the crust: Constraints from Precambrian crustally derived granites. *Geochim. Cosmochim. Acta* 60, 3717–3733.
- Vervoort, J.D., Patchett, P.J., Gehrels, G.E., Nutman, A.P., 1996a. Constraints in early Earth differentiation from hafnium and neodymium isotopes. *Nature* 379, 624–627.
- Vervoort, J.D., Patchett, P.J., Nutman, A.P., 1996b. Hf initial isotopic ratios in early Archean gneisses from Greenland. *Trans. AGU* 77, 785.
- Weaver, B.L., 1991. The origin of ocean island basalt end-member compositions: Trace element and isotopic constraints. *Earth Planet. Sci. Lett.* 104, 381–397.
- Weis, D., 1983. Pb isotopes in Ascension Island rocks: oceanic origin for the gabbroic to granitic plutonic xenoliths. *Earth Planet. Sci. Lett.* 62, 273–282.
- White, W.M., Patchett, J., Ben Othman, D., 1986. Hf isotope ratios of marine sediments and Mn nodules: evidence for a mantle source of Hf in seawater. *Earth Planet. Sci. Lett.* 79, 46–54.
- Woodhead, J.D., McCulloch, M.T., 1989. Ancient seafloor signals in Pitcairn Island lavas and evidence for large amplitude, small length-scale mantle heterogeneities. *Earth Planet. Sci. Lett.* 94, 257–273.
- Zindler, A., Hart, S.R., 1986. Chemical geodynamics. *Ann. Rev. Earth Planet. Sci.* 14, 493–571.
- Zindler, A., Hart, S.R., Frey, F.A., Jakobsson, S.P., 1979. Nd and Sr isotope ratios and rare earth element abundances in Reykjanes peninsula basalts: evidence for mantle heterogeneity beneath Iceland. *Earth Planet. Sci. Lett.* 45, 249–262.
- Zindler, A., Jagoutz, E., Goldstein, S., 1982. Nd, Sr and Pb isotopic systematics in a three-component mantle: a new perspective. *Nature* 298, 519–523.